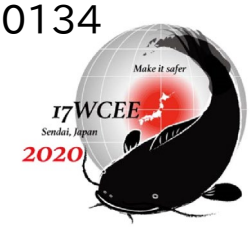

17th World Conference on Earthquake Engineering, 17WCEE
Sendai, Japan - September 13th to 18th 2020

Post Peak Simulation of RC Shear Walls with Openings based on Non-Linear FE Analysis

M. Sakurai[(1)], T. Nishida[(2)]

[(1)] *Assistant Professor, Akita Prefectural University, sakurai_masato@akita-pu.ac.jp*
[(2)] *Professor, Akita Prefectural University, tetsuya_nishida@akita-pu.ac.jp*
...

Abstract

Reinforced concrete (RC) shear walls are one of the primary seismic-resistant elements in RC buildings. However, there are many instances where it is necessary to install openings in the RC shear walls, from the aspects of building regulations, planning, and usability. RC shear walls with openings also play a role as seismic-resistant elements in RC buildings. However, the stress transfer within the wall panel is not uniform as compared to shear walls without openings. In particular, a complicated stress transferring mechanism is formed in the vicinity of the opening due to the design. Therefore, it is difficult to evaluate the seismic performance of RC shear walls with openings with sufficient accuracy using the current evaluation method according to the Japanese standard. Accordingly, it was necessary to develop an evaluation method that considers the opening configuration.

It was proven that using the modeling technique of nonlinear finite element (FE) analysis for RC shear walls with openings can be reproduced, for example, by studying the hysteresis characteristic and crack damage situation, if limited to the region up to the maximum shear capacity. However, the simulation, which focused on the reproduction of the post peak behavior, was not proposed as a reasonable modeling technique. This is because the calculation was prone to become unstable, and the reproduction of the capacity degradation behavior with the difference of the opening configuration was not reached.

The main objective of this study was to predict the seismic performance of RC shear walls analytically, calculating the failure mode, hysteresis characteristic, and deformability, to establish an evaluation method that can determine the shear strength of walls with multi-openings.

For this study, RC shear walls with openings in shear failure were examined using an FE modeling technique that can reproduce the capacity degradation behavior at the post peak. Then, parametric studies were completed for the purpose of determining the tendency analysis of shear walls with openings in shear failure, and analyzing the effect of the opening arrangement on the capacity degradation behavior in detail.

During the examination of the modeling technique of FE analysis, the validity was verified by the simulation of a past experiment, using some models on the constitutive law of the softening region of concrete as analysis variables. As a result, it was shown that the capacity degradation behavior in the experiment could be approximately reproduced by the modeling technique outlined in this paper.

During parametric analysis, it was used the opening size as a variable. The shear wall with a small opening size showed the rapid shear capacity degradation after the maximum shear, similar to the shear wall without an opening. On the other hand, in the case of a shear wall with a large opening size, because the maximum shear capacity became smaller by the effect of the opening size, the shear capacity degradation became moderate, and behaved like a column beam frame.

Keywords: RC shear walls with openings, post peak behavior, FE analysis, capacity degradation

1. Introduction

It is Japanese practice that the shear strength of reinforced concrete (RC) walls with openings is generally estimated as a factor of reduced strength of walls without openings, but having the same configuration and bar arrangement. The reduction factor is basically defined as the equivalent perimeter ratio of the openings, which is the ratio of the opening area to the total wall surface area, evaluated by the Equation (1) [1].

$$\eta = \sqrt{\frac{\sum h_{op} l_{op}}{hl}} \tag{1}$$

where, h : story height(mm), l : wall lengh including both boundary columns (mm)
h_{op}, l_{op} : opening height and opening length (mm), η : equivalent perimeter ratio of openings

However, the locations of openings also need to be considered. According to past structural test results and actual seismic damages observed on shear walls with openings, their failure mechanisms are complicated, and cannot be simply estimated by the reduction factor [2]. The reason for this complexity is that the behavior of shear walls with openings is significantly affected by the number and layout of the openings. In fact, few studies have been conducted focusing on the seismic performance of shear walls with multiple openings. The main objective of this study was to develop a reasonable evaluation method for analyzing the shear strength of RC walls with multiple openings.

Taking into account the background information mentioned above, a shear strength evaluation was proposed based on the results of static loading tests and nonlinear finite element (FE) analysis. The proposed method considered the possibility of evaluating the shear strength according to the opening position and the number of openings [3].

The experimental results indicated that the final failure mode of RC shear walls with openings was different, depending on the shape, number, and position of the openings. In particular, depending on the location of the opening, the concrete collapse of the wall panels around the opening led to the frame-like behavior of the attached column beam.

It was observed that it was very useful to the economic design if the opening characteristics (which are rich in ductility) were understood, and if the high ductility behavior (after the shear capacity was reached) was accurately evaluated and incorporated into the design. Therefore, it was important to evaluate the behavior after the shear capacity was reached for the seismic loadings, before further examination was carried out using the quantitative evaluation method for RC shear walls with openings.

Though the structural experiment was effective for the evaluation of the behavior after the shear capacity was reached, it became very difficult to establish the evaluation only from the experimental results. This was because of the high cost that existed as a result of the infinite combinations of opening shape, number of openings, and position in the wall panel. Therefore, modeling using FEM was necessary for the verification. In the past, a model with high reproducibility of hysteresis characteristics, shear capacity, and crack situation had been proposed. However, since this method did not consider the behavior after the shear capacity was reached, it was necessary to examine the connection to the experimental results in the large deformation region.

The purpose of this study was to continue the past structural experiment, carrying out the simulation using FE analysis and to construct an FE model for evaluating the behavior after the shear capacity was reached. This was followed by application of the quantitative evaluation method, after the shear capacity was reached, for the RC shear walls with openings. For this study, an FE modeling technique that can reproduce the capacity degradation behavior at post peak, for RC shear walls with openings in shear failure, was examined. Finally, parametric studies were carried out for the purpose of showing the tendency analysis of shear walls with openings in shear failure and analyzing the effect of the opening arrangement on the capacity degradation behavior in more detail.

2. Analytical Program

2.1 Analyzed Specimens

FE analysis was conducted on the RC shear walls with various opening layouts to simulate the post peak capacity of RC shear walls. A total of six test cases were analyzed. One-third sized scale models were used, to simulate the lower 2 or 2.3 stories of multi-story shear walls in medium-rise RC buildings [2,4]. Details of the section and configuration of the specimens are shown in Table 1 and Fig. 1. The variables investigated were the number and layout of the openings. Specimens WO1 and WO6 had one opening each, while Specimens WO2, WO3, WO4, and WO5 each had two openings. The two openings in Specimen WO2 were positioned close to one another, while those in Specimens WO3 and WO4 were at a distance apart, and those in Specimen WO5 were unusually located, as shown in Fig. 1. The equivalent perimeters ratios of the openings for Specimens WO1, WO2, and WO3 were equal to 0.4, while those for Specimens WO4, WO5, and WO6 were about 0.35. The mechanical properties of the materials used are listed in Tables 2 and 3.

The wall specimens were loaded using horizontal shear reversals using a 1,000 kN manual jack with a constant axial force of 442 kN, and with two vertical manual jacks of 2,000 kN capacity each. During the testing, an additional moment was also applied to the top of the specimens using vertical jacks to keep the prescribed shear-span ratio of 1.38. The loading was conducted by controlling the relative wall drift angle, R, calculated by the ratio of the height, corresponding to the measuring point of horizontal displacement at the top of the specimen, h, to the horizontal deformation, δ, i.e. R=δ/ h.

Table 1 – Specification of section

		WO1, WO2, WO3		WO4, WO5, WO6		All Specimens	
		1st story	2nd story				
Column	B×D	200×200			wall	Thickness	80
	Longitudinal bar	12-D13(p_g=3.8%)				Longitudinal bar	D6@100zigzag (ps=0.4%)
	Tie	2-D6@60 (p_w=0.53%)	2-D6@50 (p_w=0.64%)	2-D6@60 (p_w=0.53%)		Transverse bar	D6@100zigzag (ps=0.4%)
	Sub-tie	2-D6@120 (p_w=0.27%)	---------	2-D6@120 (p_w=0.27%)		bar around opening	D10
beam	B×D	150×200	150×200	150×200	*Upper 300mm of beam depth 500 has combined with an upper stab Unit: mm		
	Longitudinal bar	4D-10(p_t=0.54%)					
	Stirrup	2-D6@100(p_w=0.42%)					

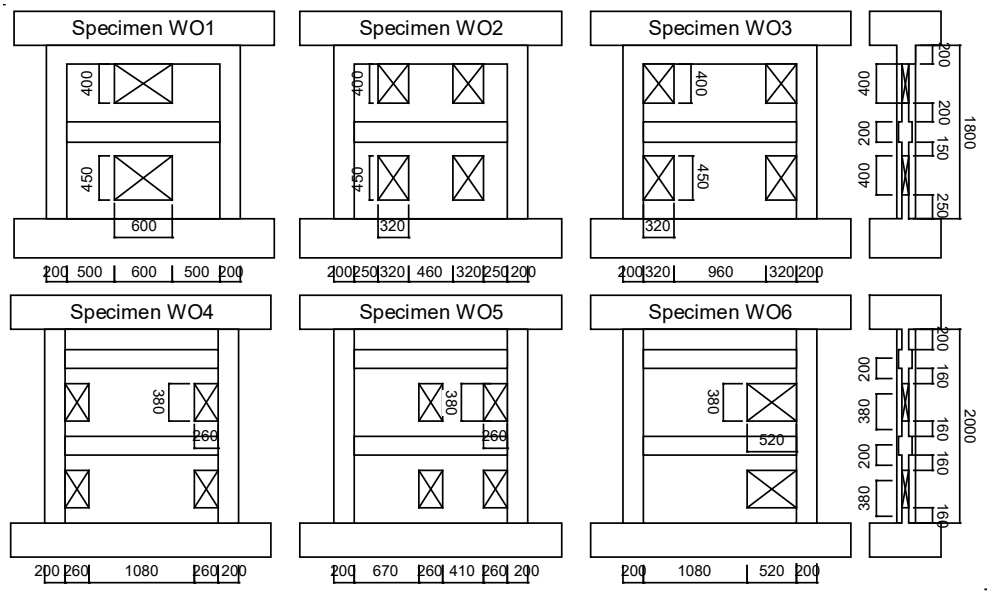

Fig. 1 – Test specimens

2.2 Analytical Model

The FE models were calibrated against the experimental results. The FE mesh layout for Specimen WO1 is shown in Fig. 2. Each node at the bottom end of the under stub had pin support to restrain vertical and lateral displacement. The elements between the loading point prescribed shear-span ratio of 1.38 and the top end of upper stub were defined as an elastic body, which is a virtual stub. A node at the top of the virtual stub was subjected to lateral displacement reversals by applying a constant initial axial force of 442 kN. During unloading, it was controlled by the forced displacement until the peak displacement of the previous cycle, and then, it was controlled by the load control, which made the load of the top node to be zero. These controls applied during the unloading were intended to prevent an unexpected displacement increase due to normal forced unloading at the top node and instability of the analysis in the large deformation region. The non-linear FE analysis software "FINAL" was used for this analysis [5].

2.3 Element Model

The mechanical properties of the material model used for the analysis are listed in Tables 2 and 3. The quadrilateral plane stress element was used for concrete. Reinforcing bars and transverse reinforcements in the wall panels stirrup of the columns and beams were accounted for by using equivalent layers with stiffness in the bar direction, superposed on the quadrilateral elements. Longitudinal reinforcing of the columns and beams were modeled by the truss elements. Further, line elements were used between the truss elements and the quadrilateral elements to reflect the bond slip behavior.

2.4 Constitutive Law of Materials

Concrete is idealized using the orthotropic model based on the strain concept. The smeared crack model for concrete elements was determined using the non-orthotopically crack model, which considered multi-directional cracking [6]. As for the stress-strain relationships of concrete until the maximum stress, a modified Ahmad model was adopted. Kupher-Gerstle's criterion [7] was applied for failure in biaxial compression and in tension-compression. Degradation of compressive strength and strain after cracking were incorporated. The

Table 2 – Mechanical properties of reinforcing steel

Steel bar		Yield strength (N/mm^2)		Young's modulus (kN/mm^2)		Ultimate strength (N/mm^2)	
		WO1-WO3	WO4-WO6	WO1-WO3	WO4-WO6	WO1-WO3	WO4-WO6
D6 (SD295A)	Wall reinforcement, tie, stirrup	336	338	211	187	565	509
D10 (SD295A)	Beam reinforcement, bar around opening	327	348	163	190	439	487
D13 (SD390)	Column reinforcement	422	405	173	185	562	595

Table 3 – Mechanical properties of concrete

Specimen	WO1		WO2		WO3		WO4		WO5		WO6	
Story	1st	2nd	1st	2nd	1st	2nd	1st	2nd	1st	2nd	1st	2nd
σ_c (N/mm^2)	32.9	29.7	34.7	29.5	34.9	28.6	28.4	26.5	26.6	26.4	26.9	24.8
F_t (N/mm^2)	2.82	2.66	2.91	2.65	2.92	2.61	2.60	2.50	2.50	2.49	2.52	2.40
E_c (N/mm^2)	26.2	26.2	26.7	25.1	26.8	24.8	24.7	24.1	24.1	24.0	24.2	23.5
ε_{c0} (μ)	4500	4500	4500	4500	4500	4500	4500	4500	4500	4500	4500	4500
Poason's ratio	0.167	0.167	0.167	0.167	0.167	0.167	0.167	0.167	0.167	0.167	0.167	0.167

compressive reduction factor was defined as a function of uniaxial compressive strength of concrete and acting normal stresses along the reinforcement directions, modeled on the basis of RC panel tests by Naganuma [8].

The purpose of this study was to clarify which model can better simulate the experimental results over the large deformation region. Generally, for FE analysis of concrete-based materials, there are many constitutive laws during which the stress is largely reduced after the maximum stress. Therefore, it tends to become unstable according to the equilibrium convergence calculation of each element in the large deformation region. Thus, to simulate the behaviors of post peak capacity over the large deformation region, analytical variables were softening zone characteristic models at stress-strain relationships of concrete as shown in Fig. 3. Analytical models Case 1, Case 2, and Case 3, used the Darwin–Pecknold model [9], modified Ahmad model [10], and Nakamura and Higai model [11], respectively, for identifying the softening zone characteristic model, as shown in Fig. 3. In the case of the Darwin–Pecknold model, for analytical model Case 1, the softening region characteristics were expressed as a straight line connecting the point at 0.2 times the maximum stress and 4 times the strain at maximum stress were obtained at the maximum stress point. Thereafter, the model was made to stop at 0.2 times the maximum stress, regardless of the strain increase. The modified Ahmad model for Case 2 was a curvilinear model that expressed the strength and deformability increase of concrete, due to the constraining effects of reinforcements by the function based on the compressive strength and reinforcement ratio of concrete. For the Nakamura and Higai model, for Case 3, the slope of the softening characteristics changed, according to the compressive strength of concrete and dimensions of the quadrilateral elements. In particular, the slope became gentle as the element dimensions were small.

In the tensile zone, the tension stiffening envelope after cracking was determined as a function of the compressive stress and reinforcement ratio proposed by Yamaguchi and Naganuma [12]. The hysteric rule on the shear stress - shear strain relationship was modeled. The shear transferring action was expressed as the average shear stress-shear strain relationship along the crack direction. The shear stress - shear strain envelope was determined as a function of the concrete strength, the amount of reinforcing steel crossing the cracks, and tensile strain perpendicular to the crack direction (Naganuma 1991). For the stress - strain relationship under stress reversals, because the unloading and reloading response of concrete is not clear, the unloading and reloading curves were represented using quadratic equations for compression and tension [13].

The bond stresses between reinforcing bars and concrete versus slip deformation relationships for line elements were represented as follows. The maximum bond stress of concrete was calculated using the AIJ

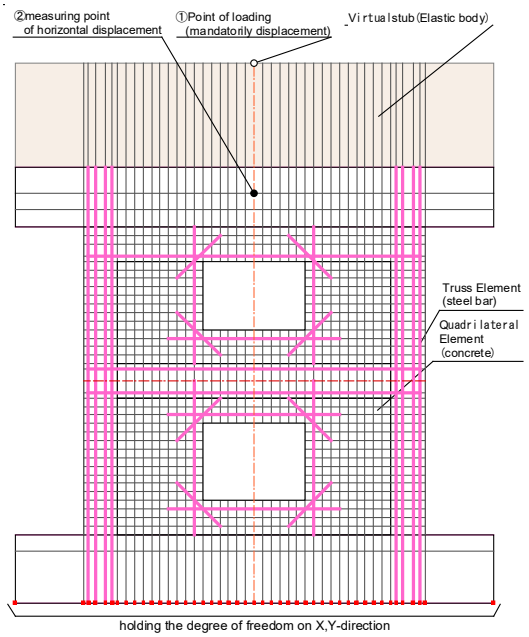

Fig. 2 – Finite element mesh layout (Specimen WO1)

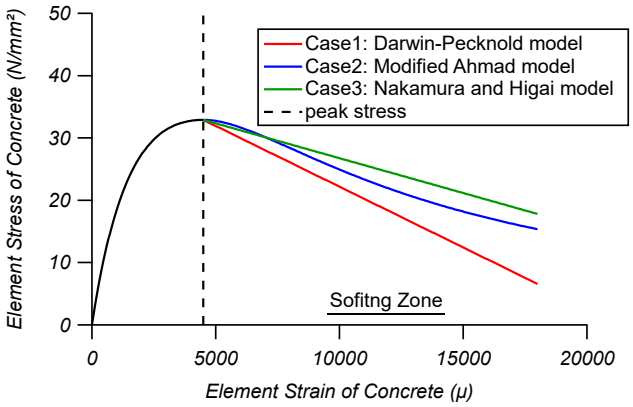

Fig. 3 – Modeling for Softing Zone

design standard for RC buildings, based on the inelastic displacement concept [14] and the sliding at the maximum bond stress, which was assumed to be 1.0 mm. The reversal loading model for bond behavior was represented by the modified Elmorsi model [15].

The material model used for reinforcing bars was a plasticity model, based on the Von Mises model failure surface with associated plastic rule. The stress-strain curve of the reinforcing bars under stress reversal was idealized by Ciampi's model [16], and the isotropic hardening rule was adopted as the hysteresis model.

Because the constitutive law used for FE analysis did not consider the degradation of member stiffness coupled with the drying shrinkage of concrete, the calculated elastic E_c modulus, strain at compressive strength, and tensile strength of concrete were reduced according to the literature [17].

3. Comparison Analysis with Test

3.1 Hysteresis Loops

The analytical results on the shear force versus displacement relationships for all specimens are compared with the experimental results in Fig. 4. The analytical backbone curves agreed well with the experimental results until an R of 1/200 rad.. It was expressed to the maximum shear strengths during the analysis at the drift angle, R, of 1/200 rad for each specimen. For the experimental results, the shear capacity of Specimens WO1, WO2, and WO5 gradually decreased after the maximum shear capacity. However, for the analytical results, a similar tendency was observed for analytical models of Case 1, Case 2, and Case 3. In particular, analytical model Case 1 indicated the best correlation with the experimental results. On the other hand, the experimental results of Specimens WO3, WO4, and WO6 indicated a tendency to decrease significantly after the maximum shear capacity. For Specimens WO3 and WO6, there was a rapid decrease in the strength, which was considered to be due to the existence of an opening adjacent to the boundary column, and particularly for Specimen WO4, a slip fracture in shear occurred in the wall panel.

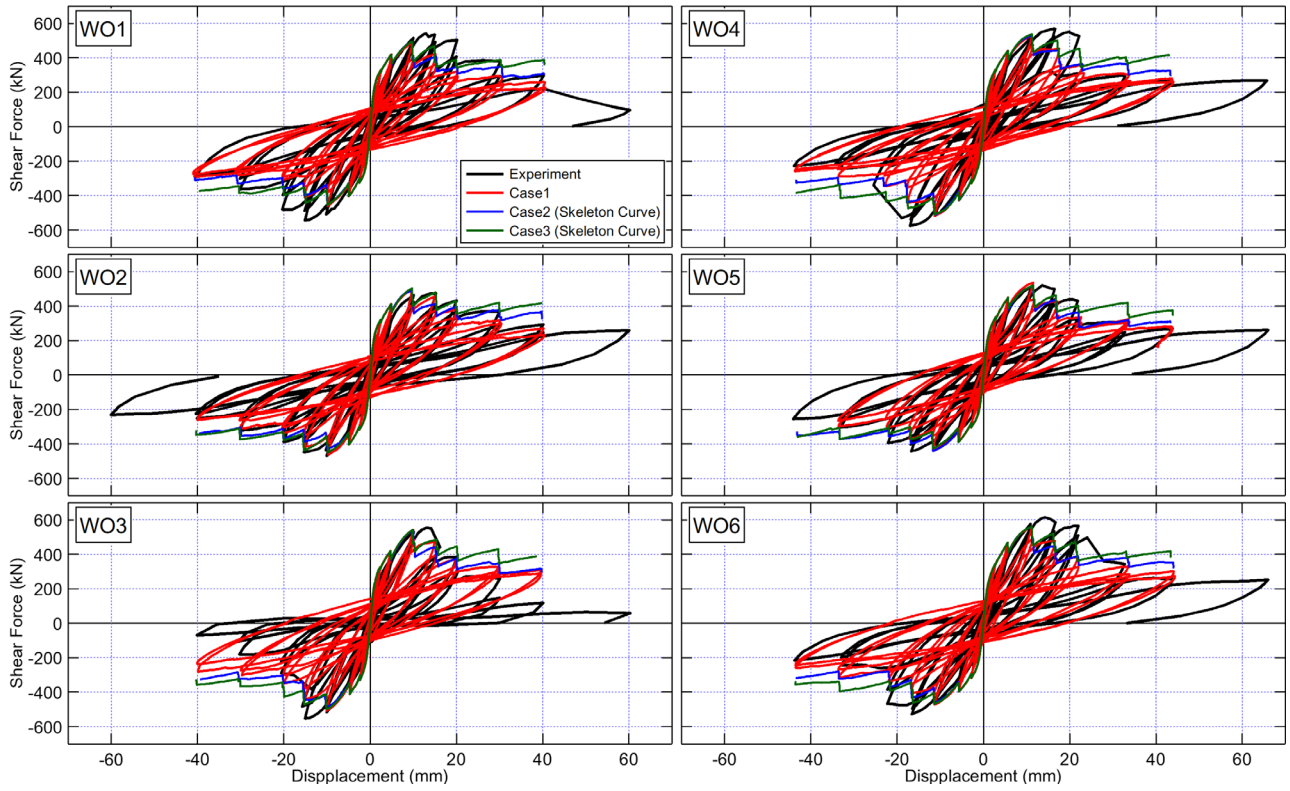

Fig. 4 – Comparison with the analytical and the experimental in hysterisis loop

The analytical results of the shear force versus the drift angle relationships, after the maximum shear capacity was reached for all specimens, are compared with the experimental results in Fig. 5. In the figure, the vertical axis represents the rate of decrease in the shear capacity, obtained by dividing the shear force Q at the peak displacement of each loading cycle, by the maximum capacity Q_{max} of the specimens. For Specimens WO1, in which the opening was arranged in the center, and WO2, in which the opening was arranged symmetrically, the tendency of degrading the shear capacity after the maximum shear by the analysis corresponds well with the experimental result. Conversely, the analytical results for Specimens WO3, WO4, and WO6, which showed a rapid decrease in shear capacity after the maximum shear and slip fracture during the experiment, did not follow the behavior of the rapid decrease in shear capacity, as shown by the trend in Fig. 4.

In addition,in the positive and the negative loading of Specimens WO3 and WO4, and in the negative loading of WO6, the discrepancy between the experimental and analytical results became significant, and the corresponding accuracy decreased at δ_Q/δ_{Qmax} = 1.5, which was the next cycle of the loading cycle at the maximum bearing capacity, and δ_Q/δ_{Qmax} = 2.0, which was the next subsequent cycle. However, for Specimen WO5, in which the shear capacity degradation behavior became gentle in the experiment, the analytical rate of degradation of the shear capacity during the positive loadings was highly reproducible. Thus, for a shear wall, in which the opening is located at a zone where compressed struts can be concentrated and where brittle fracture is foreseen, the proposed modeling method indicated poor agreement with the experiments.

The analysis results of analytical model Case 1, which was a Darwin–Pecknold model, indicated good agreement with the shear capacity reduction rate shown in the experiments. Analytical model Case 2, a modified Ahmad model, tended to underestimate the rate, whereas, analytical model Case 3, a Nakamura and Higai model, further tended to underestimate the rate. One reason for this was that the relationship between the element stress and the strain of concrete materials for analytical model Case 1 indicated the largest slope of the softening region, when compared with the other two models. This was consistent with the behavior of strength reduction in the experiment.

According to these results, it was difficult to accurately reproduce the failure process for the specimens that exhibited a rapid decrease of the shear capacity (after the maximum was reached) or for the model with the unusually located opening. However, the modeling method proposed using the Darwin–Pecknold model did roughly grasp the tendency of the capacity decrease, as caused by the variance of the opening condition for the RC shear wall with openings.

3.2 Damage Situation

The crack diagram of each specimen during the final loading cycle for analytical model Case 1 are shown in Fig. 6.

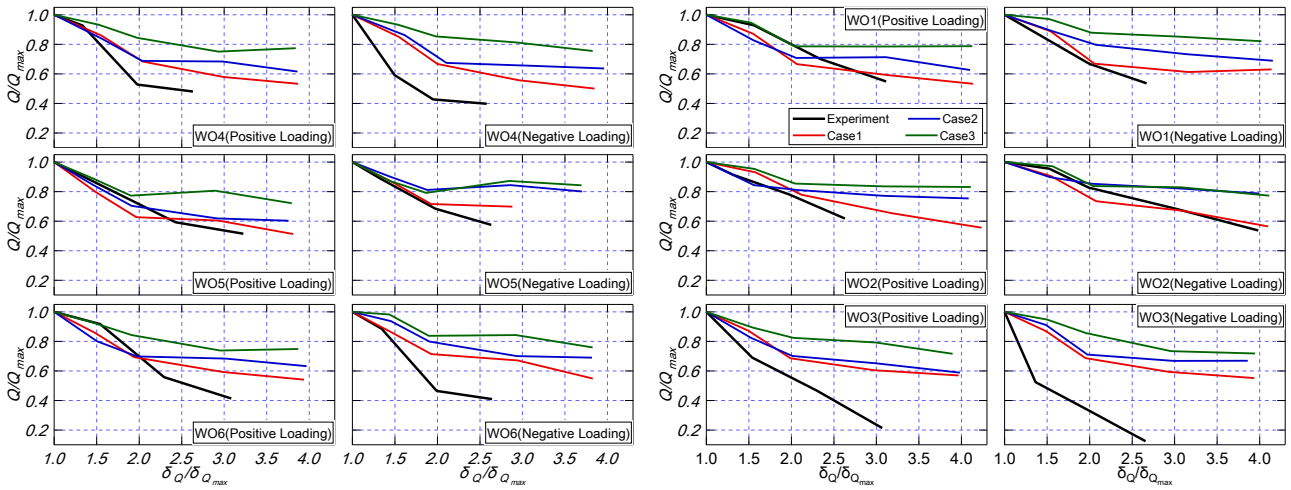

Fig.5 – Raito of maximum capacity in large deformation region

For each specimen, the analytical results roughly identified the generation position of the crack in the experiment, and the symptoms of the concrete collapse were confirmed in the wall board around the opening of each layer. Furthermore, in the analysis of the wall panels, there was damage concentrated between the openings and the boundary columns, similar to the experimental results. However, the reproducibility of the analysis was poor in regard to the spalled concrete at the boundary columns found in the 2nd story. Further, the slip fracture at the top of the boundary columns for Specimen WO3, and in the wall panels of the 1st story in Specimen WO4, were not reproducible by the analysis. Analytical models Case 2 and Case 3 showed similar crack damage situations.

Even though the reproducibility of local fracture, such as damage to the boundary column and slip fracture was not sufficient, this study confirmed that analysis using the proposed modeling method can reproduce crack generation position and concrete collapse position for the loading test result.

4. Parametrical Study

It was shown that the behavior, after the maximum shear capacity of RC shear walls members was reached, can be simulated by the modeling technique mentioned in the preceding section. Based on this result, parametric analysis was carried out for the purpose of the clarification of the behavior for the large deformation region of RC shear walls with openings. In this section, the results of the analysis are described.

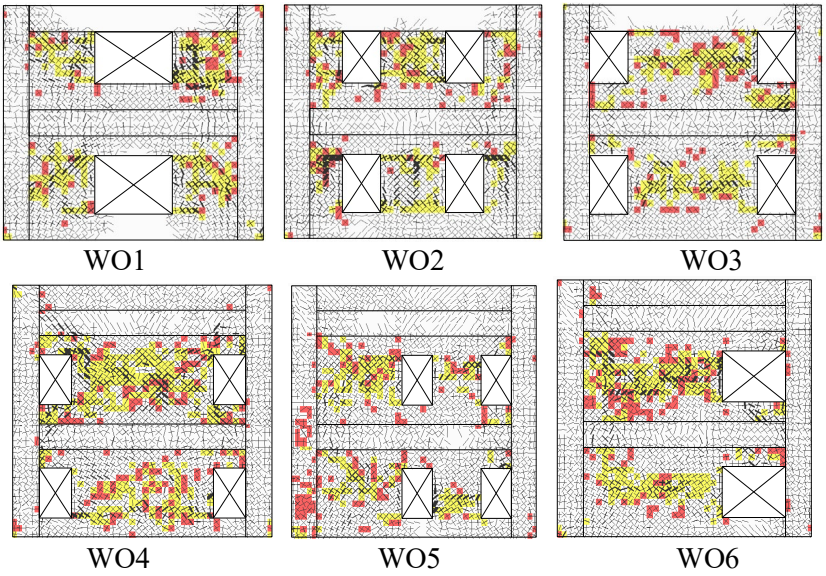

Fig.6 – Damage situation

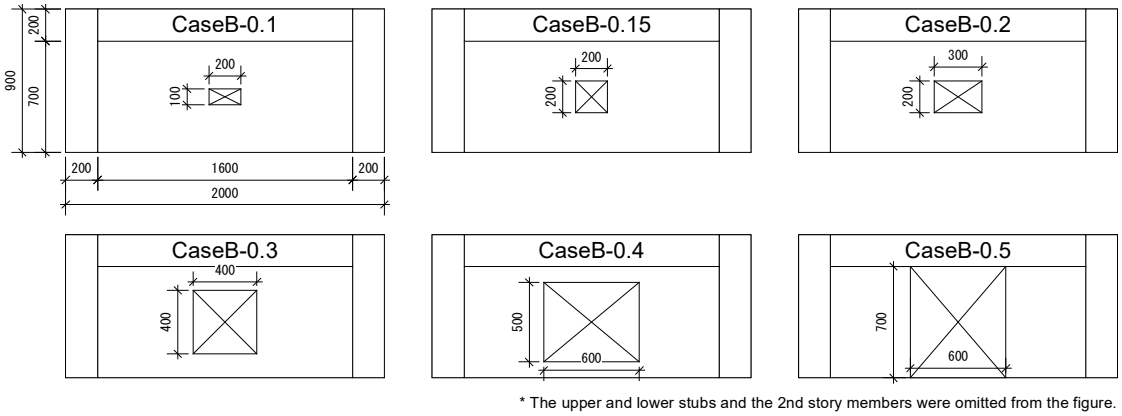

* The upper and lower stubs and the 2nd story members were omitted from the figure.

Fig.7 – Detail of Analytical Model

4.1 Analyzed Specimens

Analytical details are shown in Fig. 7, and the material property of concrete and steel are listed in Tables 4 and 5. For the analytical model shape, the opening was placed in the center of the wall panel, with reference to Specimen WO1. The analytical model was made for all seven cases, and the shear wall without arranging the opening was named analytical model Case A, and the shear wall with an opening at the center was named analytical model Case B. For analytical model Case B, the analytical variable was the size of the opening, and the ratio of the opening area to the wall panel was set to be 0.1, 0.15, 0.2, 0.3, 0.4, and 0.5. Considering the experimental values, the material property was made to be 25 N/mm^2 for the concrete, and 1.1 times of the standard strength for each steel material as listed in Tables 4 and 5. All of the material constitutive laws used for modeling and analysis were the same, as introduced in the previous section.

4.2 Analytical Results

A comparison of the load-deformation relationship between analytical model Case A, the shear wall without an opening, and that of Case B, the shear wall with an opening, are shown in Fig. 8. The hysteresis characteristics of the models, with the equivalent perimeter ratios of opening of 0.1, 0.15, and 0.2 in analytical

Table 4 – Material Property for Concrete

Story	σ_c (N/mm^2)	F_t (N/mm^2)	E_c (N/mm^2)	ε_{c0} (μ)	Poason's ratio
1st	25	2.41	23.6	4500	0.167

Table 5 –Material Property for Steel

Steel bar		Yield Strength (N/mm^2)	Young's modulus (kN/mm^2)
D6(SD295A)	wall reinforcement, tie, stirrup	324.5	205
D10(SD295A)	beam reinforcement, bar around opening	324.5	205
D13(SD390)	column reinforcement	379.5	205

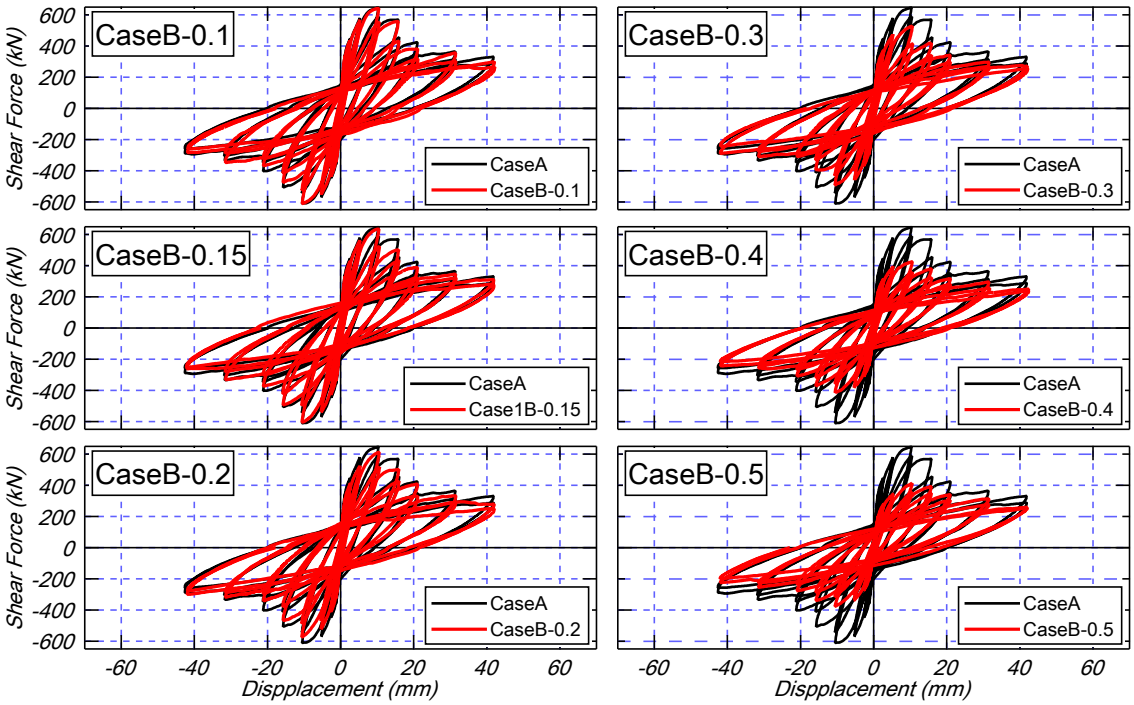

Fig.8 – Hysterisis Loop

model Case B, were almost the same as those in Case A. However, for the hysteresis characteristics of ratios 0.3, 0.4, and 0.5 in analytical model Case B, the loading cycles that reached the maximum shear were the same, although the maximum shear capacities were different. In particular, the decrease of the maximum shear capacities became significant in line with the increase of the equivalent perimeter ratios of the opening. Furthermore, it was indicated that the degradation of shear became small regardless of the displacement increase.

4.3 Internal Stress Transmission

The principal compressive stress distributions of concrete elements at the drift angle R of 1/133 rad for each specimen are shown in Fig. 9. The amount of deformation of the specimens shape is shown at a magnification of 10 times in the figure.

For all specimens, there was an area of large deformation and small compressive stress found in the wall panel, and it was presumed that the stress transmission decreased with the damage, for example, crack and collapse of concrete.

It was considered that the uniform strut was formed in the entire wall board for analytical model Case A (shear wall without openings) and analytical model Case B-0.1 (with small equivalent perimeter ratios of opening). Conversely, for the analytical model where the opening circumference ratio of Case B-0.3 and Case B-0.5 was large, the stress was transmitted to the wing wall of the opening side, and the compression strut was formed in each wing wall of the opening side. It was proven that the complicated compression strut was formed by the effect of the damage. In addition, this tendency was significant in analytical model Case B-0.5 (with the largest opening area), and especially, the stress concentration was confirmed at the opening end of each layer. Because the area of the wing wall decreased with an increase in the opening area, due to an increase in the equivalent perimeter ratios of opening, it was presumed that higher compressive stress occurred in the wing wall. In addition, regarding the 1st and 2nd stories beams, the stress increase stress was found to be caused by

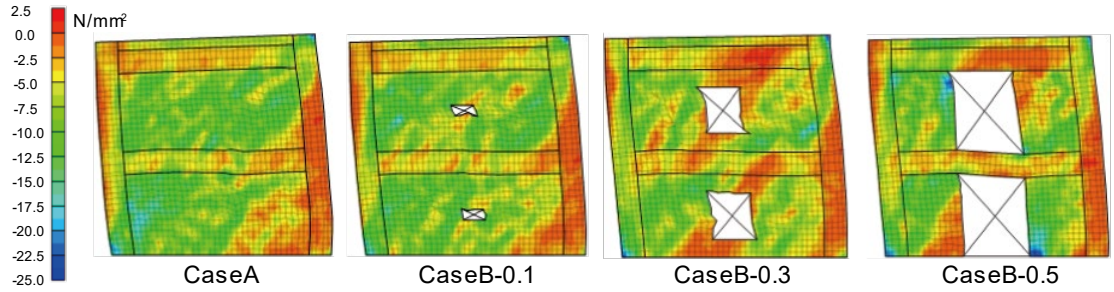

Fig.9 – Minimum principal stress distribution

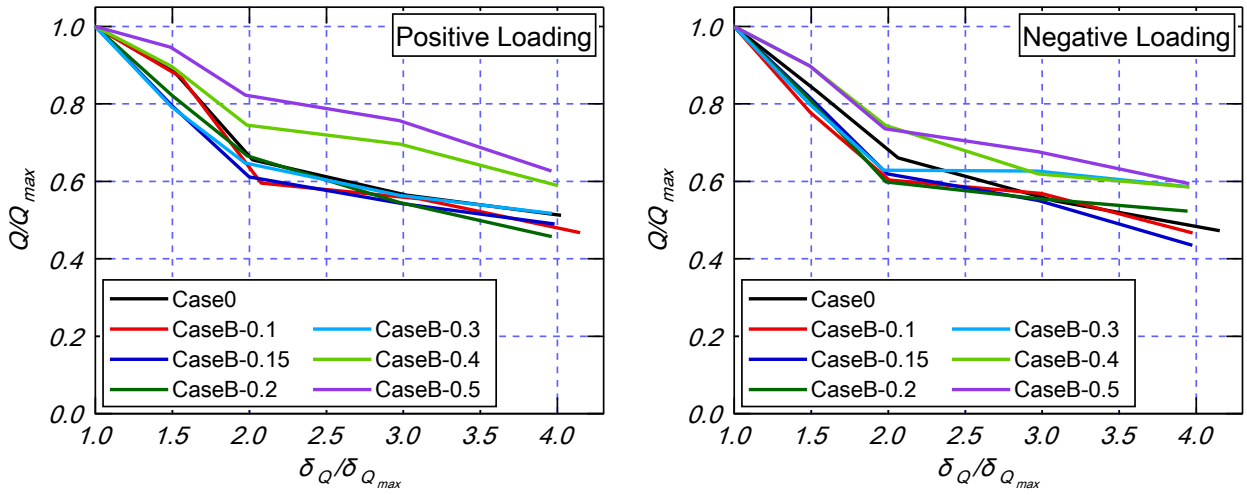

Fig.10 – Raito of maximum capacity in large deformation region

the decrease of the area of the hanging wall and the spandrel wall above and below the beam. As in the case of the wing wall, and the deformation of the beam in analytical model Case B-0.5 became significant.

4.4 Behavior after maximum shear

The relationship between the ratio of shear capacity degradation and displacement after the maximum shear capacity in the positive loadings is shown in Fig. 10. The vertical axis in the figure shows the ratio of shear capacity degradation, obtained by dividing the shear capacity Q at the peak displacement of each loading cycle, by the maximum shear force Q_{max} of the analytical models. For the horizontal axis, the peak displacement δ_Q of each loading cycle was also normalized by the displacement δ_{Qmax}, at the maximum shear.

Among the analytical models, Case A, which was a shear wall without opening, and Case B-0.1, which had a small opening, displayed almost the same ratio of shear capacity degradation with the increase of displacement. For the analytical models Case B-0.15, Case B-0.2, and Case B-0.3, the ratio of shear capacity degradation at $\delta_Q/\delta_{Qmax} = 1.5$, when the loading cycle of R = 1/133 rad, was about 10% different from that of Case A. However, after $\delta_Q/\delta_{Qmax} = 2.0$, when R = 1/100 rad, the ratio of shear capacity degradation showed a tendency similar to that of Case A. On the other hand, for analytical models Case B-0.4 and Case B-0.5, which had the equivalent perimeter ratios of opening 0.4 and 0.5, the ratio of shear capacity degradation was smaller than in the other models, and it was confirmed that the ratio of shear capacity degradation tended to be smaller with an increase in the opening size.

From the above results, it was found that the tendency of shear capacity degradation (after the maximum shear capacity) was similar to that of Case A (which was a shear wall without opening), for models with equivalent perimeter ratios of opening of 0.1, 0.15, and 0.2. This might have been because the maximum shear capacity was almost the same as that of a shear wall without opening (and that with openings) with equivalent perimeter ratios of 0.1 to 0.2, respectively. Further, the difference in the minimum principal stress distribution was small.

Conversely, for analytical models with a large opening size, the shear capacity degradation for large deformation was smaller than that of a shear wall without openings. This was because the shear capacity of the wing wall was relatively small, even though the shear capacity degradation occurred from the increased damage of the wing wall with the displacement increase, and it was considered that the strength garnered from the frame of beams and columns after the maximum shear relatively contributes the most. It was hypothesized that this tendency became significant when the equivalent perimeter ratios were larger.

5. Conclusion

For this study, an FE modeling technique that can reproduce the capacity degradation behavior at the post peak was examined for RC shear walls with openings in shear failure. Parametric studies were completed for the purpose of understanding the tendency analysis of shear walls with openings in shear failure. Further, the effect of the opening arrangement on capacity degradation behavior was analyzed in detail. The following conclusions were drawn:

(1) Analytical model Case 1, using the Darwin–Pecknold model, indicated values closer to the experimental values for each specimen, and the tendency of shear capacity degradation after the maximum shear was well dealt with. In Case 2, using the modified Ahmad model, the shear capacity degradation tended to be underestimated after the maximum shear was reached, and in Case 3, using the Nakamura and Higai model, the tendency to be underestimated became more remarkable.

(2) Even when the constitutive law model for any softening region was used, the failure properties (such as slip fracture and rapid degradation of shear capacity) could not be reproduced, and the reproduction accuracy was difficult to assess.

(3) From the analysis results, using the opening size as a variable, the shear wall with a small opening size showed the rapid shear capacity degradation after the maximum shear, similar to the shear wall without an opening. On the other hand, in the case of a shear wall with a large opening size, because the maximum shear capacity became smaller by the effect of the opening size, the shear capacity degradation became moderate, and behaved like a column beam frame.

Acknowledgment

This work was supported by JSPS KAKENHI Grant Numbers JP17K14759. The authors would like to thank Shota Miura who finished his master's degree from our research group for technical assistance with the analysis.

References

[1] Architectural Institute Japan (2018), *AIJ standards for Structural Calculation of Reinforced Concrete Structures,* (In Japanese)

[2] Sakurai. M, Kuramoto, H., T., Matsui, and Akita, T. (2008): Seismic performance of RC shear walls with multi-openings, *Proceedings of 14th World Conference on Earthquake Engineering*, Paper-ID12-03-0071.

[3] Sakurai. M, Kuramoto, H. and T.Matsui (2009): an Evaluation method of shear strength for RC shear walls with multi-openings, *Transactions of AIJ. Journal of Structural and Construction Engineering*, Vol.77, No.679, 1445-1453. (In Japanese)

[4] Sakurai, M., T., Matsui, Suzuki, K., and Kuramoto, H. (2008): Influence of opening layouts affecting to seismic performance for RC shear walls on multi-openings, *Proceedings of the Japan Concrete Institute*, Vol.30, No.3, 421-426.

[5] ITOCHU Techno-Solutions Corporation (2009). FINAL/11 HELP (In Japanese)

[6] Naganuma, K., Kurimoto, O. and Eto, H. (2001): Finite element analysis of reinforced concrete walls subjected to reversed cyclic and dynamic loads, *Transactions of AIJ. Journal of Structural and Construction Engineering*, No.544. 125-132. (In Japanese)

[7] Kupfer, B., and Gerstle, H. et al. (1973): Behavior of concrete under biaxial stress, *Journal of the engineering mechanics division*, 853-866.

[8] Naganuma, K. (1991): Nonlinear analytical model for reinforced concrete panels under in-plane stresses, *Transactions of AIJ. Journal of Structural and Construction Engineering,* No.421, 39-48. (In Japanese)

[9] Darwin,D.and Pecknold,D.A.(1977): Nonlinear biaxial stress-strain law for concrete, *Journal of the Engineering Mechanics Division*, ASCE, Vol.103, No.EM2, pp.229-241.

[10] Naganuma, K. (1995): stress-strain relationship for concrete under triaxial compression, *Transactions of AIJ. Journal of Structural and Construction Engineering,* No.474, 163-170. (In Japanese)

[11] H. Nakamura, T. Higai (1999): Compressive fracture energy and cracture zone length of concrete, *Seminar on Post-peak Behavior of RC Structures Subjected to Seismic Load*, JCI-C51E, Vol.2, 259-272.

[12] Yamaguchi, T. and Naganuma, K. (1990): Experimental study on mechanical characteristics of reinforced concrete panels subjected to in-plane shear force, *Transactions of AIJ. Journal of Structural and Construction Engineering*, No.419, 77-86. (In Japanese)

[13] Naganuma, K. and Ohkubo, M. (2000): An analytical model for reinforced concrete panels under cyclic stresses, *Transactions of AIJ. Journal of Structural and Construction Engineering,* No.536, 135-142. (In Japanese)

[14] Architectural Institute Japan. (1999): *Design Guidelines for Earthquake Reinforced Concrete Buildings Based on Inelastic Displacement Concept*. (In Japanese)

[15] Elmorsi, M., Kianoush, M. R. and Tso, W. K. (2000): Modeling bond-slip deformations in reinforced concrete beam-column joints, *Canadian Journal of Civil Engineering*, Vol.27, 490-505.

[16] Ciampi, V. et al. (1982): Analytical model for concrete anchorages of reinforcing bars under generalized excitations, *Earthquake Engineering Research Center,* Report No. EERC-82/83, paper.

[17] Sakurai, M, T.Matsui, and Kuramoto, H. (2009): Non-linear FEM analysis for RC shear walls with multi-openings, *Transactions of AIJ. Journal of Structural and Construction Engineering,* No.639, 915-923. (In Japanese)

